Identifying effective forecast horizon for real-time reservoir operation under a limited inflow forecast

Tongtiegang Zhao,[1,2] Dawen Yang,[1] Ximing Cai,[2] Jianshi Zhao,[1] and Hao Wang[1,3]

Received 2 March 2011; revised 3 October 2011; accepted 13 December 2011; published 26 January 2012.

[1] The use of a streamflow forecast for real-time reservoir operation is constrained by forecast uncertainty (FU) and limited forecast horizon (FH). The effects of the two factors are complicating since increasing the FH usually provides more information for decision making in a longer time framework but with increasing uncertainty, which offsets the information gain from a longer FH. This paper illustrates the existence of an effective FH (EFH) with a given forecast, which balances the effects of the FH and FU and provides the maximum information for reservoir operation decision making. With the assumption of a concave objective function, a monotonic relationship between current operation decision and ending storage is derived. Metrics representing the error resulting from a limited forecast relative to a perfect forecast are defined to evaluate reservoir performance. Procedures to analyze the complicating effect of FU and FH and to identify EFH are proposed. Results show that: (1) when FH is short, FH is the dominating factor for determining reservoir operation, and reservoir performance exhibits a quick improvement as FH increases; (2) when FH is long, the inflow information may be too uncertain to guide reservoir operation decisions and FU becomes the dominating factor; and (3) at a medium FH, reservoir performance depends on the complicating effects of FU and FH and EFH locates with a certain balanced level of FU and FH. The statistical characteristics of EFH are illustrated with case studies with deterministic forecast and ensemble forecast. Moreover, the impacts of temporal correlation of FU, inflow variability, evaporation loss, and reservoir capacity on EFH are explored.

Citation: Zhao, T., D. Yang, X. Cai, J. Zhao, and H. Wang (2012), Identifying effective forecast horizon for real-time reservoir operation under a limited inflow forecast, *Water Resour. Res.*, *48*, W01540, doi:10.1029/2011WR010623.

1. Introduction and Background

[2] As advances in weather forecasting, hydrologic modeling, and hydro-climatic teleconnections have significantly reduced streamflow forecast uncertainty and prolonged the forecast horizon, streamflow forecasts are now a more promising tool for improving reservoir operation efficiency [*Carpenter and Georgakakos*, 2001; *Faber and Stedinger*, 2001; *McCollor and Stull*, 2008; *Sankarasubramanian et al.*, 2009a]. In recent years, various optimization and simulation models have been developed to exploit streamflow forecasts for reservoir decision making [e.g., *Yao and Georgakakos*, 2001; *Ajami et al.*, 2008; *Huang and Hsieh*, 2010; *Valeriano et al.*, 2010]. However, Applications of streamflow forecasts to reservoir operation are constrained by their limited length. A meaningful forecast horizon (FH) is usually shorter than the reservoir operation horizon. For example, reservoir flood control operations may last several months, while a streamflow forecast is only available several weeks in advance. The practical length of a streamflow forecast is also limited by the complicating relationship between forecast uncertainty (FU) and forecast horizon (FH), i.e., the longer the forecast horizon, the more complete the information for decision making, but the larger the forecast uncertainty [*Simonovic and Burn*, 1989; *Maurer and Lettenmaier*, 2003, 2004].

[3] In previous reservoir operation studies, the importance of reducing FU has been illustrated by using both an operational forecast with actual reservoir systems [e.g., *Georgakakos et al.*, 1998; *McCollor and Stull*, 2008; *Sankarasubramanian et al.*, 2009a] and a synthetic forecast with hypothetical reservoir systems [e.g., *Georgakakos and Graham*, 2008; *Graham and Georgakakos*, 2010; *Zhao et al.*, 2011]. Meanwhile, most studies assumed that the available FH was as long as the operation horizon and did not consider the complicating effect of FU and FH. However, a few previous publications have shed light on the issue. By employing a Kalman filter forecast technique, *Simonovic and Burn* [1989] illustrated the existence of an empirical FH threshold, and argued that a FH longer than the threshold would not contribute to reservoir performance. More recently, *You and Cai* [2008a] presented both a theoretical and a numerical framework to determine the optimal forecast horizon for a given decision horizon, which is defined

[1]Institute of Hydrology and Water Resources, Department of Hydraulic Engineering, Tsinghua University, Beijing, China.
[2]Ven Te Chow Hydrosystem Laboratory, Department of Civil and Environmental Engineering, University of Illinois at Urbana Champaign, Champaign, Illinois, USA.
[3]Department of Water Resources, China Institute of Hydropower and Water Resources, Beijing, China.

0043-1397/12/2011WR010623

as the initial periods in which decisions are not affected by forecast data beyond the forecast horizon. Furthermore, *You* [2008] addressed the dual problem of *You and Cai* [2008a], i.e., how far the actual decision is away from the optimal one under a given forecast with a limited horizon.

[4] Following *You and Cai* [2008a] and *You* [2008], the current study develops metrics to evaluate reservoir release decisions under a limited forecast and procedures to analyze the effect of FU and FH and to identify EFH. To conduct the analysis, a fixed ending storage is specified for a reservoir operation problem. With this realistic setting, a monotonic relationship between reservoir release in the current period and ending storage is derived with a concave objective function. With the monotonic relationship, metrics representing the error resulting from a limited forecast relative to a perfect forecast are defined. Following that numerical experiments based on synthetic forecasts are designed to analyze the complicating effect of FH and FU and to illustrate the procedures to identify the effective forecast horizon (EFH), beyond which FH increase will not contribute to reservoir operation efficiency. The statistical characteristics of EFH are illustrated with case studies with deterministic forecast and ensemble forecast. Moreover, the impacts of temporal correlation of FU, inflow variability, evaporation loss, and reservoir capacity on EFH are explored.

2. Evaluation Metrics of Limited Inflow Forecast for Reservoir Operation

[5] Section 2 first discusses FU and FH with a particular reservoir operation optimization model, and then provides evaluation metrics of a limited inflow forecast for reservoir operation.

2.1. Problem Formulation

[6] Consider a reservoir operation problem with an operation horizon of N periods and denote the variables as follows:

i the index of time periods;
s_i reservoir storage at the end of period i;
q_i reservoir inflow at period i;
x_i forecast of period i reservoir inflow;
r_i period i reservoir release decision;
$f_i()$ period i reservoir utility function;
$\underline{s}$ the minimum reservoir storage;
$\overline{s}$ the maximum reservoir storage;
$\underline{r}$ the minimum reservoir release;
$\overline{r}$ the maximum reservoir release;
d discount ratio of reservoir utility;
l loss ratio of reservoir storage;
s_0 the initial reservoir storage;
s_T the target storage at the end of reservoir operation horizon (N);
s'_T the target storage at the end of reservoir inflow forecast horizon (H).

[7] Based on the aforementioned variables and the selection of reservoir release r_i as decision variable, the multiple-period reservoir operation optimization model can be formulated as follows [*Yeh*, 1985; *Labadie*, 2004]:

$$\max \quad \sum_{i=1}^{N} \frac{1}{(1+d)^{i-1}} f_i(r_i) \tag{1a}$$

$$s.t. \quad \begin{cases} (1-l)s_{i-1} + q_i - r_i = s_i (i = 1, \ldots, N) & (1b) \\ \underline{s} \le s_i \le \overline{s} & (1c) \\ \underline{r} \le r_i \le \overline{r} & (1d) \\ s_N = s_T & (1e) \end{cases}$$

Equation (1a) denotes the reservoir operation objective and it is defined as the sum of discounted reservoir utility, which is a function of reservoir release r_i and assumed concave (i.e., diminishing marginal utility or $f''(r_i) \le 0$, for example, willingness to pay for one more unit of water is high in drought periods and it decreases as water scarcity abates) in this paper [*Draper and Lund*, 2004; *You and Cai*, 2008a, 2008b]; (1b) is the water balance equation which illustrates the conservation of mass between reservoir storage, inflow and release; (1c) is the storage capacity constraint; (1d) is the release capacity constraint; and (1e) is the ending storage constraint.

[8] Reservoir operation optimization shown in equation (1) is an ideal case and the underlying assumption is that reservoir inflows through the operation horizon N are perfectly known (i.e., no limitation on FH and FU) (Figure 1). In real-world reservoir operation, the inflow information is available only within a limited horizon H [*You and Cai*, 2008a; *You*, 2008] and involves uncertainties [*Simonovic and Burn*, 1989; *Ajami et al.*, 2008; *Graham and Georgakakos*, 2010]:

$$x_i = q_i + \varepsilon_i, \tag{2}$$

where ε_i is a random variable indicating forecast uncertainty of period i ($i \le H$) reservoir inflow.

[9] To bridge the gap between the operation horizon N and the forecast horizon H, real-world reservoir operation typically employs a rolling horizon approach (Figure 1), i.e., (1) making the release decision for the forecast horizon (FH = H) with a limited forecast; (2) implementing the current release decision (DH = 1); (3) move to the next

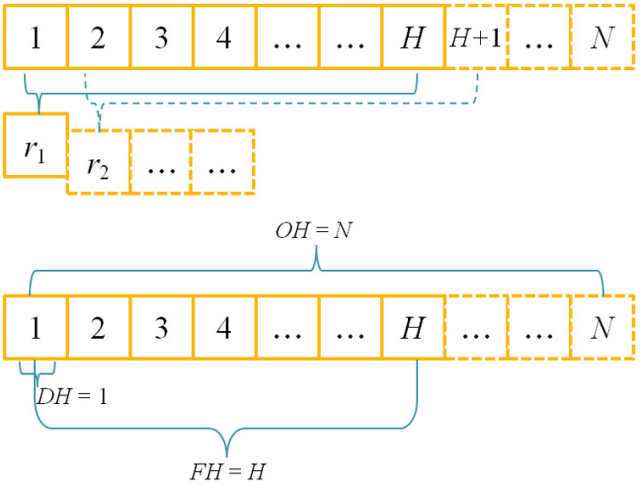

Figure 1. Schematic of reservoir operation rolling horizon decision making and its operation horizon, forecast horizon, and decision horizon.

period and repeat (1) and (2) with updated inflow forecast and reservoir storage until the end of operation horizon [*Simonovic and Burn*, 1989; *Martinez and Soares*, 2002; *Zhao et al.*, 2011].

[10] In the rolling horizon approach, decision horizon (*DH*, how long the generated decision is implemented), forecast horizon (FH, how long the inflow can be predicted), and operation horizon (*OH*, how long the reservoir operation is targeted) are important issues (Figure 1). As the inflow forecast can update period by period in real-time reservoir operation, *DH* is usually set as 1 (i.e., only the current period decision is treated as final and decisions in future periods will be updated with the new forecast). FH depends on the forecast technology and *OH* is set equal to FH, although the original *OH* (equation (1)) is determined by inflow variability and reservoir characteristics (e.g., a seasonal reservoir has an *OH* of several months and an annual reservoir has an *OH* of one year).

[11] The reservoir optimization operation model for rolling horizon decision making can be formulated as follows:

$$\max \quad \sum_{i=1}^{H} \frac{1}{(1+d)^{i-1}} f_i(r_i) \tag{3a}$$

$$s.t. \begin{cases} (1-l)s_{i-1} + x_i - r_i = s_i (i = 1, \ldots, H) & (3b) \\ \underline{s} \le s_i \le \overline{s} & (3c) \\ \underline{r} \le r_i \le \overline{r} & (3d) \\ s_H = s'_T & (3e) \end{cases}$$

Equation (3) represents a practical reservoir operation model, which is different from equation (1) in: (1) x_i contains forecast uncertainty; (2) the operation horizon is H; (3) the user-specified ending storage is s'_T (the target end storage, which is differentiated from s_T used in equation (1)). With the forecast updated and s'_T specified in each period, the rolling horizon approach can be employed to determine real-time reservoir releases.

[12] The practical model (equation (3)) can generate a release sequence $[r'_1, r'_2, \ldots, r'_H]$ within FH while only the current decision r'_1 is implemented (*DH* is 1, Figure 1) and subsequent decisions will be obtained by rerunning the practical model with an updated inflow forecast through the rolling horizon process. For reservoir operation applications, the rolling horizon approach generally exhibits superior performance to the climatology scenario based stochastic approach, especially in extreme hydrologic conditions [*Martinez and Soares*, 2002; *Sankarasubramanian et al.*, 2009a]. For the comparability of decision making through the rolling horizon process, this paper focuses on one single period and investigates the gap between r'_1 (the local optimal decision with a limited forecast, equation (3)) and r^*_1 (the global optimal decision with a perfect forecast, equation (1)).

2.2. Monotonicity Property and Reservoir Release Bounds

[13] One direct question from the rolling horizon approach is how the generated local optimal decision can approximate the global optimal decision, i.e., the gap between r^*_1 and r'_1. Since s'_T indicates the trade off between water use within FH and water use beyond FH and affects r'_1 (i.e., ending storage effect, equation (3)), another question is what effect s'_T exerts on the gap between r'_1 and r^*_1. This paper addresses the second question first and illustrates a monotonic relationship between s'_T and r'_1.

[14] The theorem is as follows: Given a predetermined forecast horizon FH and inflow forecast $[x_1 \quad x_2 \quad \ldots \quad x_H]$, if the reservoir release utility function $f_i()$ exhibits a diminishing marginal utility property (i.e., concavity and $f''_i() < 0$), then r'_1 underlying a given s'_T will not increase if s'_T increases.

[15] The proof of this theorem is given in Appendix A. This theorem illustrates a monotonic ending storage s'_T effect on first period decision r'_1. For rolling horizon reservoir operation, this monotonic relationship generally suggests that the current release decision r'_1 will not increase if we set a higher s'_T (i.e., to save more water for periods beyond FH). It is important to note that the monotonicity dependence relationship has been studied in supply chain management [e.g., *Veinott*, 1964; *Huang and Ahmed*, 2010]; this paper introduces the relationship to reservoir operation and extends it by considering the effects of utility discount and storage loss (Appendix A).

[16] A direct corollary of the monotonicity theorem is that: r'_1 is bounded by $r'_{1,u}$ (upper bound, corresponding to $s'_T = \underline{s}$) and $r'_{1,l}$ (lower bound, corresponding to $s'_T = \overline{s}$). In general, $r'_{1,u}$ implies the release decision under the most optimistic expectation of future streamflow, as total inflow plus initial storage are scheduled to be used up within FH. Alternately, $r'_{1,l}$ implies the release decision under the most pessimistic expectation of future streamflow and that storage and inflow are planned to be saved as much as possible for periods beyond FH. For real-time reservoir operation, when practical values of $\underline{s}$ and $\overline{s}$ are given, these two releases bounds $r'_{1,u}$ and $r'_{1,l}$ can be used to determine the range of reservoir release decisions under a given streamflow forecast (Figure 2).

[17] Based on the monotonicity property of r'_1 and the two release bounds $r'_{1,u}$ and $r'_{1,l}$, we can analyze the gap between r^*_1 and r'_1 (i.e., the optimality of reservoir operation decision with a limited forecast). The gap between r^*_1 and r'_1 is bounded and can be represented by the gaps between

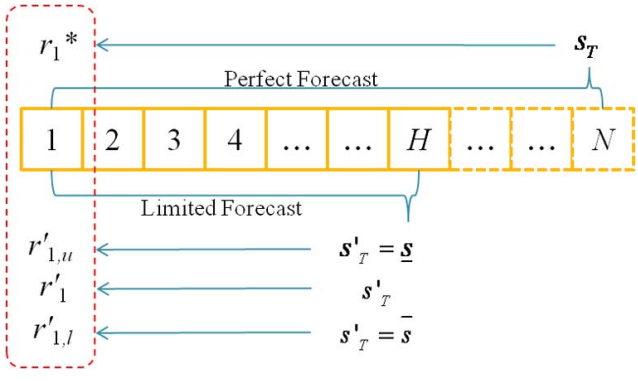

Figure 2. The optimal first period release decision r^*_1 of the ideal model and the upper and lower bound for the first period release decision r'_1 of the practical model.

r_1^* and $r'_{1,u}$ and between r_1^* and $r'_{1,l}$. Three error bound indices are derived:

$$\mathrm{EBR} = r'_{1,u} - r'_{1,l}, \tag{4}$$

$$\mathrm{EBU} = r'_{1,u} - r_1^*, \tag{5}$$

$$\mathrm{EBL} = r_1^* - r'_{1,l}. \tag{6}$$

Error bound range (EBR) is the difference between $r'_{1,u}$ and $r'_{1,l}$, or rather, the variation in the range of r'_1. upper error bound (EBU) and lower error bound (EBL) indicate the error bound of the most optimistic and pessimistic expectation of future streamflow, respectively.

[18] For these three indices, EBR is applicable to real-time reservoir operation for the determination of the release range. As r_1^* is obtained through perfect information of reservoir inflow (not possible in real-time reservoir operation), EBU and EBL are retrospective analysis indices with the assumption that the inflow process has already been realized and release decisions $r'_{1,u}$ and $r'_{1,l}$ were made prior to inflow realization. This paper is, thus, a retrospective analysis of real-time reservoir operation and applies EBR, EBU and EBL to diagnosing the optimality of release decision under a limited forecast. In the following section 3, this paper will investigate EBR, EBU and EBL by varying FH, FU, streamflow variability, and reservoir characteristics. Considering the difficulty of obtaining an analytic optimal solution for the multiple period reservoir optimization operation model (equations (1) and (3)), numerical experiments with a hypothetical reservoir are adopted in the subsequent analysis.

3. Numerical Experiments to Detect Effective Forecast Horizon

[19] Section 3 sets up a hypothetical reservoir system with an *OH* of 100 periods to study effect of FH and FU on reservoir operation decision making. Synthetic forecast generators are used to generate forecast characterized with FH and FU; numerical experiments are conducted to analyze the complicating effect of FH and FU through the defined evaluation metrics (EBR, EBU, and EBL).

3.1. Numerical Experiment Design

[20] The reservoir system is characterized by storage capacity s and storage loss ratio l. s is defined as the maximum active storage (i.e., the difference between the maximum and minimum storage). The operation of the reservoir system consists of three steps: streamflow generation, synthetic forecast generation, and reservoir operation decision making.

[21] 1. Streamflow generation: the Thomas-Fiering model is adopted for streamflow generation [*Loucks et al.*, 1981]

$$q_{i+1} = \mu + \rho_{\mathrm{flow}}(q_i - \mu) + \sqrt{1 - \rho_{\mathrm{flow}}^2}(\mu C_v)\omega. \tag{7}$$

In equation (7), μ is the mean generated streamflow and is set as 1; ρ_{flow} is the temporal correlation of the streamflow; C_v is the coefficient of variability; and ω is a random number with the standard Gaussian distribution. The minimum generated streamflow is set as 0 (i.e., nonnegativity).

[22] 2. Synthetic forecast generation: the reservoir inflow forecast is generated by exerting a random disturbance to the generated streamflow [e.g., *Lettenmaier*, 1984; *Datta and Burges*, 1984; *Graham and Georgakakos*, 2010], as shown in equation (2). To represent the "increasing uncertainty with forecast horizon" property of streamflow forecast [*Maurer and Lettenmaier*, 2003, 2004; *Zhao et al.*, 2011], forecast uncertainty ε_i is assumed to fit a symmetric Gaussian distribution with the variance linearly increasing with i (i.e., the forecast lead-time):

$$\varepsilon_i \sim N(0, \varsigma_i^2) \tag{8}$$

$$\varsigma_i^2 = \min(i\sigma^2, \mu^2 C_v). \tag{9}$$

Equations (8) and (9) indicate that the variance of forecast uncertainty ς_i^2 is not greater than that of streamflow $\mu^2 C_v$. In addition to σ that determines the magnitude of single-period uncertainty in the forecast, ρ_{error} is introduced to characterize the temporal correlation of multiple-period uncertainties, which is illustrated in detail in Appendix B.

[23] 3. Reservoir operation decision making: the ideal model in equation (1) and the practical model in equation (3) are employed for reservoir operation decision making. To reduce the initial-storage effect on reservoir operation, s_0 in both equation (1) and equation (3) are set as $s/2$ (middle level of active storage). s_T in equation (1) is also set as $s/2$ while s'_T in equation (3) is set as $\underline{s}$ or $\overline{s}$ to obtain the maximum or minimum release decision with a limited forecast (Figure 2). The single period utility function is set as

$$f_i(r_i) = \ln(r_i). \tag{10}$$

In equation (10), the natural logarithm function is a concave utility function with constant price elasticity equal to 1, which has been used in previous economic studies [e.g., *Booker and O'Neill*, 2006]. With the ideal model (equation (1)) and the generated streamflow, r_1^* can be determined; and with the practical model (equation (3)) and the generated forecast sequences, $r'_{1,u}$ and $r'_{1,l}$ can be obtained. The optimization models (equations (1) and (3)) are solved by General Algebraic Modeling System (GAMS) [*Brooke et al.*, 1998].

[24] This paper will analyze error bounds using Monte Carlo simulations and design three categories of five experiments with different parameter combinations to diagnose the effect of FH and FU (characterized by σ, ρ_{error}, and H), streamflow variability (characterized by C_v), and reservoir characteristics (characterized by l and s) on reservoir operation decision making. The parameter values of the five experiments are summarized in Table 1. As the utility discount can affect long-term reservoir operation and is not as important in real-time reservoir operation, d in equations (1) and (3) is set as zero.

[25] Experiment 1 diagnoses the effect of forecast horizon (FH) and forecast uncertainty (FU) and is taken as the baseline among the 5 experiments. By changing one parameter

Table 1. Parameter Values in the Numerical Experiments.

Experiment Parameters		Streamflow		Forecast			Reservoir	
		C_v	ρ_{flow}	σ	ρ_{error}	H	l	S
Forecast horizon and uncertainty	Experiment 1 (σ, H)	0.3	0.4	0.00–0.10	0	5–50	0.00	2.0
Forecast horizon and uncertainty	Experiment 2 (ρ_{error})	0.3	0.4	0.00–0.10	*−0.5,0.5*	5–50	0.00	2.0
Streamflow variability	Experiment 3 (C_v)	*0.1–0.5*	0.4	0.00, 0.10	0	5–50	0.00	2.0
Reservoir characteristics	Experiment 4 (l)	0.3	0.4	0.00, 0.10	0	5–50	*0.00–0.10*	2.0
Reservoir characteristics	Experiment 5 (S)	0.3	0.4	0.00–0.10	0	5–50	0.00	*1.0,10.0*

at a time from experiment 1, the effects of the other parameters are studied. Experiment 2 changes ρ_{error} from 0 to −0.5 and 0.5 to explore the effect of temporal correlation of single period FUs. Experiment 3 deals with various C_v ranging from 0.1 to 0.5 to study the reservoir operation under different streamflow variability levels. Experiment 4 takes the loss ratio varying from 0.00 to 0.10 and analyzes reservoir operation with different trade-off conditions between current and future water usage. Experiment 5 studies the effect of reservoir storage capacity by adjusting storage capacity to a smaller value (1.0) and a larger value (10.0) than experiment 1. This paper conducts 100 numerical simulations with randomly generated reservoir inflow and inflow forecasts for each of the parameter combinations present in Table 1. EBR, EBU, and EBL are calculated for each simulation and their average value and standard deviation are used to analyze the complicating effect of FH and FU on reservoir operation.

3.2. Effect of Forecast Uncertainty and Forecast Horizon

[26] Experiment 1 studies the effect of FH and FU on reservoir operation by taking the various H from 5 to 50 and σ from 0.00 to 0.10. The values of the three error bound indices (EBR, EBU, and EBL) are given in Figures 3a, 3b, and 3c, respectively. The average values of EBR, EBU, and EBL all decrease and converge to zero as FH increases; the standard deviation of EBR first increases and then decreases with FH; the standard deviation of EBU and EBL decreases with FH and then converges to a stable value depending on FU.

[27] Since both the average value and standard deviation of EBR ($r'_{1,u} - r'_{1,l}$) converge to zero (Figure 3a), the range of operation decisions underlying an inflow forecast will decrease as FH increases, and will end with zero (i.e., no variation with release decisions) when FH is long enough [*You and Cai*, 2008a; *You*, 2008]. Meanwhile, FU exerts little effect on EBR and the values of EBR remain quite stable under different values of FU. EBR exhibits low variability with a short FH or a long FH, and peaks at a medium FH (Figure 3a). This can be explained as follows: (1) when FH is short, the inflow information is too limited and there is little flexibility for reservoir operation decisions, which results in a large value of EBR. For example, when FH = 1, $r'_{1,u} = s_0 + \tilde{q}_1 - \underline{s}$, $r'_{1,l} = s_0 + \tilde{q}_1 - \overline{s}$, EBR $= \overline{s} - \underline{s}$; (2) When FH is long, there is more information but it is less reliable (Figures 3b and 3c), and consequently, this narrows the range of reservoir operation release decisions; and (3) At a medium FH, there is more inflow information than case (1) and more reliable information than case (2) to support trade-off analysis between current and future water use, which induces a large variability of EBR among different simulations.

[28] A longer forecast horizon provides more information for decision making in a longer time frame but it does so with a larger uncertainty. Figures 3b and 3c show that there exists an effective forecast horizon (EFH) beyond which prolonging FH will not contribute to a decrease in the error bound, and standard deviation of EBU (EBL) converges to a value depending on FU. Considering that "EBR = EBU + EBL", the different converging performances of the standard deviation of EBR, EBU and EBL

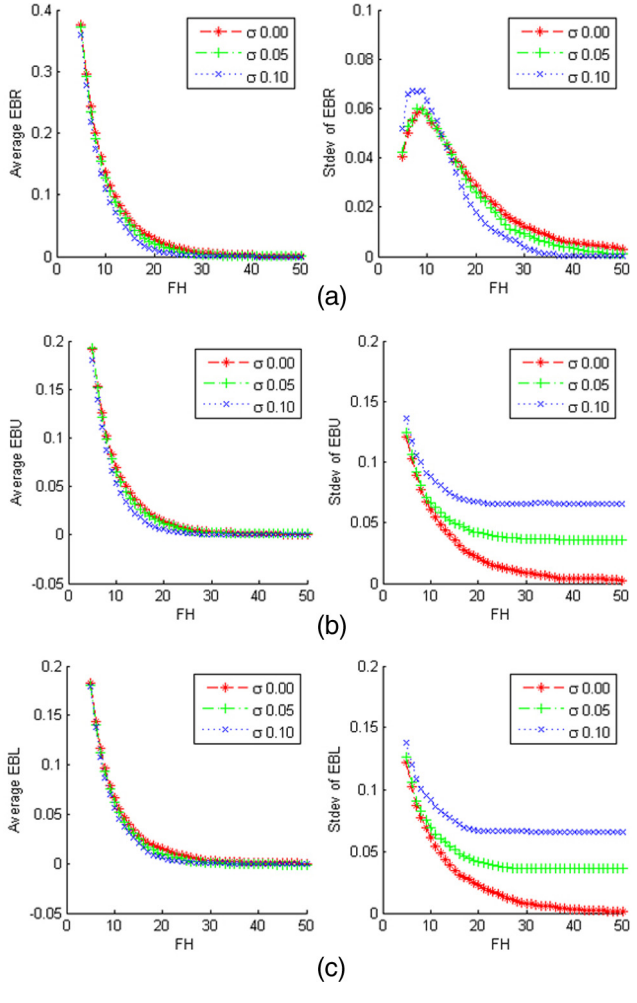

Figure 3. (a) Mean and standard deviation of EBR with FU and FH. (b) Mean and standard deviation of EBU with FU and FH. (c) Mean and standard deviation of EBL with FU and FH.

suggest that: (1) r'_1 will converge to a value as FH increases ($r'_{1,u}$ and $r'_{1,l}$, the upper and lower bounds of r'_1, will converge to the same value) [*You and Cai*, 2008a; *You*, 2008], but that value may not reach the optimal level (r^*_1) due to the effect of FU; (2) a larger FU induces a larger variability in the gap between r'_1 and r^*_1 across the various simulations. In reservoir operation analysis, the EFH concept has been discussed by *Simonovic and Burn* [1989], who applied operational forecasts to real-time reservoir operation. By simulating reservoir operation under different FU levels, Figures 3b and 3c illustrate that a larger FU induces a shorter EFH. For example, it takes about 20 periods when FU = 0.10 for EBU or EBL standard deviation to converge, about 30 periods when FU = 0.05; and longer than 50 periods when FU = 0.00 (i.e., forecast involves no uncertainty).

[29] In summary, Figures 3a, 3b, and 3c show that: when FH is short, the error bound is primarily controlled by FH and EBR, EBU and EBL exhibit a quick decrease as FH increases. When FH is long, the control factor on the error bound switches to FU, because the inflow information can be too uncertain to guide reservoir operation; in this case, although EBR becomes zero (despite FU) and there is no information to differentiate EBU from EBL (Figure 3a), EBU and EBL both exhibit a larger variability under a larger FU (Figure 3b and 3c). At a medium length of FH, the gap between r'_1 and r^*_1 depends on the complicating effect of FU and FH, i.e., less but more reliable versus more but less certain inflow information. More specifically, the EFH stays with a certain medium level due to the FU increase induced by a longer FH which, in turn, offsets the information gain (which reduces error bound) from the FH increase (Figure 3b and 3c).

[30] Experiment 2 investigates the impact of the temporal correlation between single period FU on the error bounds under various levels of FH, including the negative correlation (Figure 4, $\rho_{error} = -0.5$) and the positive correlation (Figure 5, $\rho_{error} = 0.5$). Comparing Figures 4 and 5 to Figures 3a, 3b, 3c, one can observe that: (1) ρ_{error}, either positive or negative has a trivial effect on the average values of EBR, EBU and EBL but a significant effect on the standard deviation of the error metrics; (2) a negative ρ_{error} results in a smaller standard deviation, while a positive ρ_{error} induces a high standard deviation. It is worthwhile to note that ρ_{error} will not change the magnitude of single period FU but instead will change the overall FU over the entire FH. Single period FU will be offset by the uncertainties from other periods under negative correlation and single period FUs will cumulate under a positive correlation, e.g., assuming a Gaussian distribution of ε_1 and ε_2, when $\mathrm{var}(\varepsilon_1) = 1$ and $\mathrm{var}(\varepsilon_2) = 1$, if $\mathrm{corr}(\varepsilon_1, \varepsilon_2) = -0.5$ then $\mathrm{var}(\varepsilon_1 + \varepsilon_2) = 1$ and if $\mathrm{corr}(\varepsilon_1, \varepsilon_2) = 0.5$ then $\mathrm{var}(\varepsilon_1 + \varepsilon_2) = 3$. The narrowed range of EBR, EBU and EBL standard deviation under a negative ρ_{error} and the expanded range under a positive ρ_{error} suggests that the overall FU over all periods specified by FH can have considerable effect on the optimality of reservoir operation decision [*Zambelli et al.*, 2009]. With the same single period FU level, the forecast with a smaller error correlation results in lower overall FU and consequently more efficient reservoir operation.

3.3. Effect of Streamflow Variability

[31] Experiment 3 examines the impact of different streamflow variability levels. Figure 6 displays the values of EBR, EBU, EBL from the case of $\sigma = 0.00$. As can be seen, a higher C_v involves a smaller average value of EBR with a faster convergence rate. This implies that with higher streamflow variability, lengthening FH becomes more efficient in reducing the decision range (EBR). In the case of $\sigma = 0.10$ (Figure 7), the trends of average value and standard deviation of EBR, EBU and EBL with FH are similar to that under the case with $\sigma = 0.00$, and EFH becomes

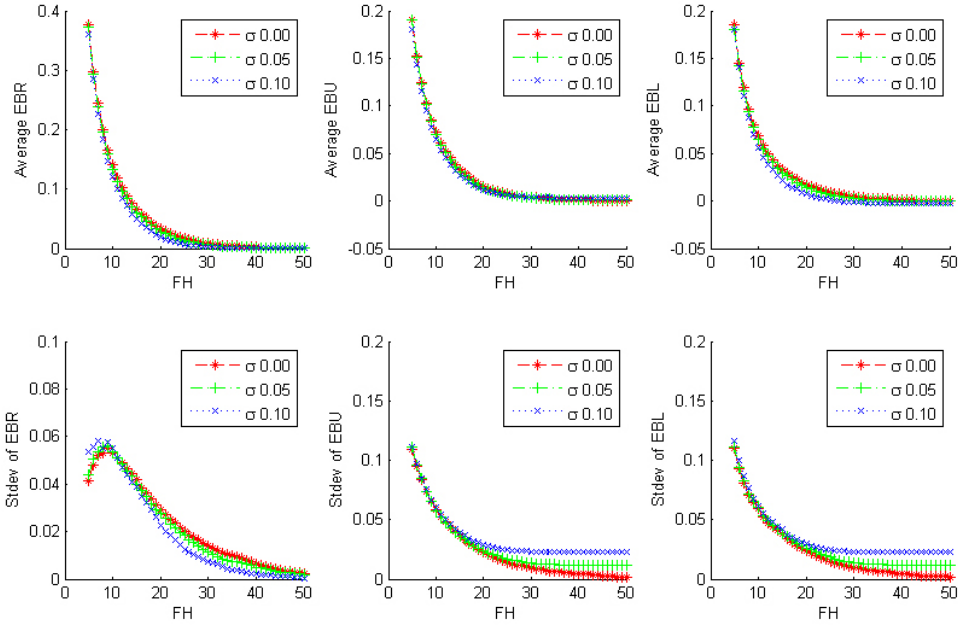

Figure 4. Forecast uncertainty temporal correlation's effect on error bounds ($\rho_{error} = -0.5$).

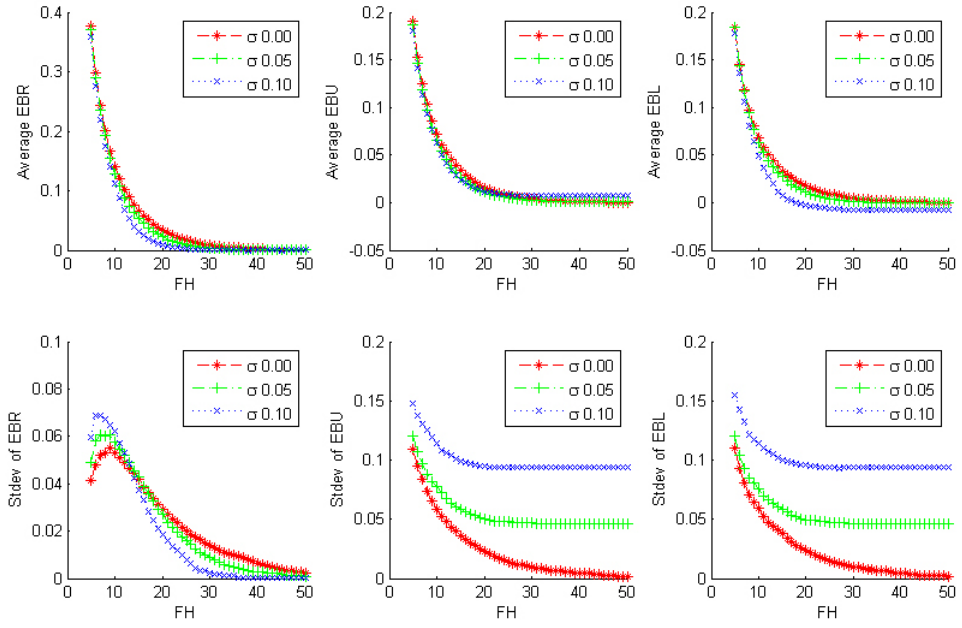

Figure 5. Forecast uncertainty temporal correlation's effect on error bounds ($\rho_{error} = 0.5$).

shorter. While it seems counterintuitive that to obtain a low-error bound, a longer FH is needed when reservoir inflow exhibits lower variability (Figure 6 and Figure 7), but with a fixed storage capacity, a reservoir system can regulate the inflow with a lower C_v through a longer time range [*Vogel and Stedinger*, 1987]. In other words, low variability allows for the exploring for the optimal solution in a longer timeframe. As a result more information can be obtained for decision making, and the uncertainty is still not too high to dominate the decision. As shown in Figure 6, with a low C_v, both the average value and standard deviation of EBU and EBL exhibit a slow convergence rate with FH.

[32] Some differences between EBU and EBL under different C_v levels are observed: EBL has a slightly larger standard deviation than EBU as C_v increases, and the difference between r_1^* and $r'_{1,u}$ is smaller than that between r_1^* and $r'_{1,l}$. This suggests that a small s'_T can induce a lower error bound (i.e., to use more water within the FH, equation (3)). The implication of this result is: if the reservoir is less effective in regulating the highly variable inflow (i.e., C_v is large), to release more water for current use is more beneficial.

3.4. Effect of Reservoir Characteristics

[33] Experiment 4 studies the effect of storage loss on reservoir operation. The results under $\sigma = 0.00$ and

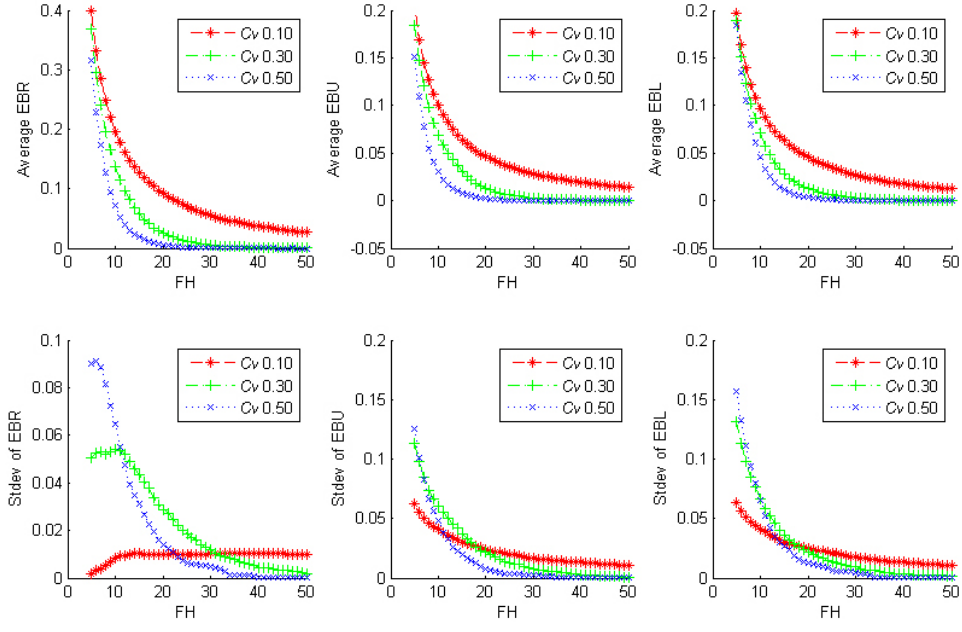

Figure 6. Streamflow variability's effect on error bounds when $\sigma = 0.00$.

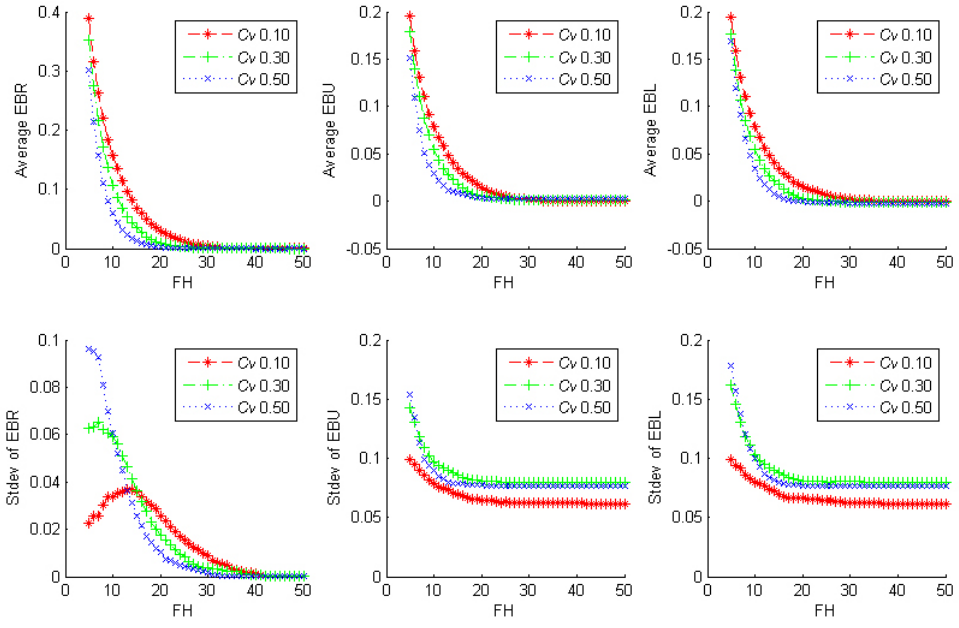

Figure 7. Streamflow variability's effect on error bounds when $\sigma = 0.10$.

$\sigma = 0.10$ are shown in Figure 8 and Figure 9, respectively. Figure 8 shows that EBL exhibits an increasingly higher average value and standard deviation than EBU as the loss ratio increases. This implies that as the loss ratio increases, it becomes more beneficial to set a lower end storage and to use more water in preceding periods [*You and Cai*, 2008b; *You*, 2008]. With high storage loss conditions, a reservoir is less effective at regulating inflow and inflow information becomes less important. When comparing EBU and EBL convergence under different storage loss ratios, EFH becomes shorter as the storage loss ratio becomes higher. The $\sigma = 0.10$ case (Figure 9) is similar to the $\sigma = 0.00$ case, except that the composite of FU and storage loss causes both the average value and the standard deviation of EBU and EBL to converge to a nonzero value.

[34] Experiment 5 examines reservoir operation under both a smaller ($s = 1.0$, Figure 10) and a larger ($s = 10.0$, Figure 11) storage capacity than experiment 1 ($s = 2.0$, Figure 3). As $s/(\mu C_v)$ indicates reservoir regulation capability of inflow variability [*Vogel and Stedinger*, 1987], a larger $s/(\mu C_v)$ allows the reservoir to regulate the inflow in a longer time range. This corresponds to a longer FH. With

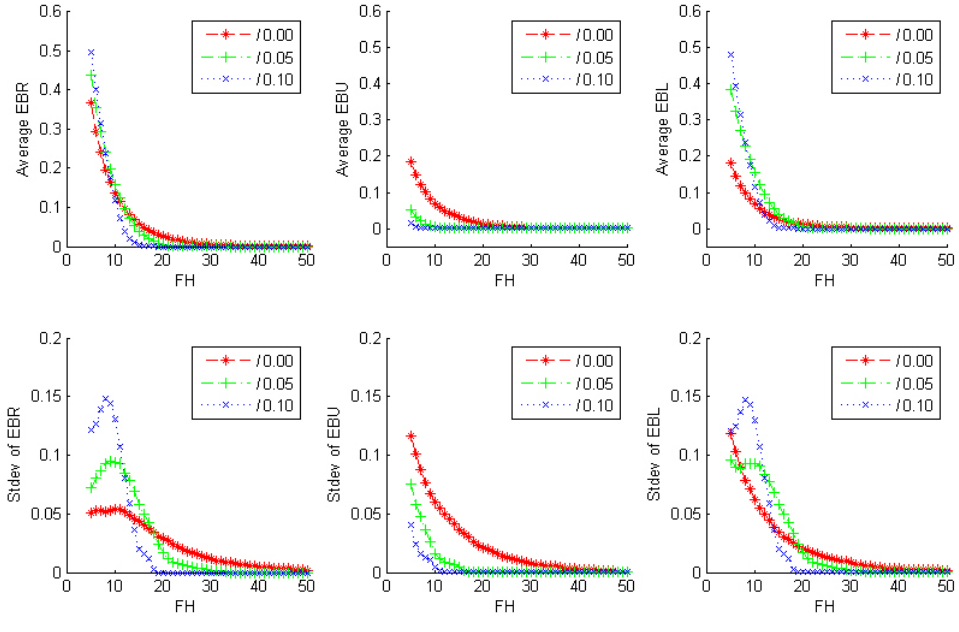

Figure 8. Loss ratio's effect on error bounds when $\sigma = 0.00$.

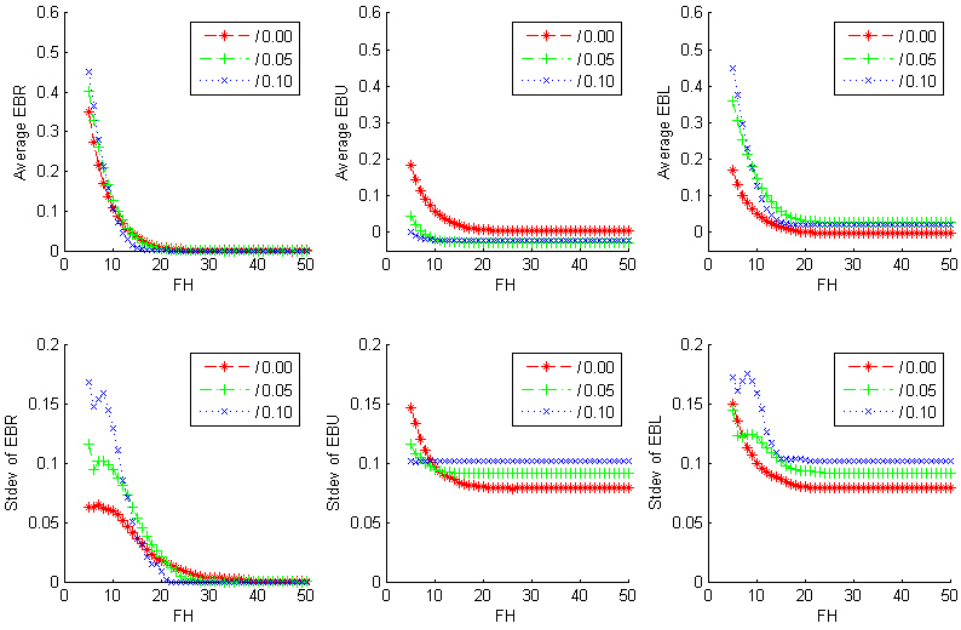

Figure 9. Loss ratio's effect on error bounds when $\sigma = 0.10$.

a smaller storage capacity (Figure 10), the trends of EBR, EBU, and EBL are similar to those with $s = 2.0$, while the magnitude of the error bounds decreases and EFH becomes shorter. This can be explained by the lower regulation capability of a smaller reservoir with a given inflow variability. In this situation, the impact of the forecast, no matter if it is perfect or subject to error, is limited, and the difference of the impact between the perfect and the imperfect forecasts is small. Thus, the error bounds defined by this difference are small, and it is not necessary to have a long EFH. For the extreme case, $s = 0$, all the error bounds are zero and the EFH is zero (i.e., for reservoirs with no storage capacity, the release is equal to the inflow and forecast may not be needed).

[35] In the case of $s = 10.0$, the minimum FH is set as ten to prevent the infeasibility of the practical model due to the generated low-flow conditions. As shown in Figure 11, the mean values of EBR, EBU, and EBL all decrease with FH, but they do not converge within the first 50 periods. This implies that with a larger $s/(\mu C_v)$, a longer FH is needed to utilize storage regulating inflow variability, thus reducing the error bound. It is important to note that with a large $s/(\mu C_v)$, the storage constraint becomes less active in the optimization model [*Booker and O'Neill*,

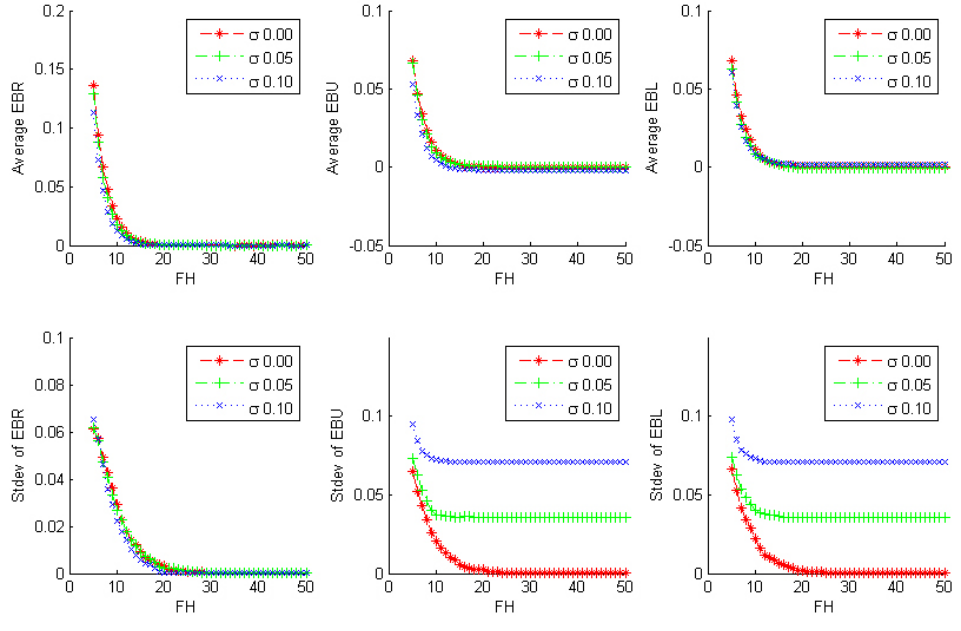

Figure 10. Reservoir storage capacity's effect on error bounds (s = 1.0).

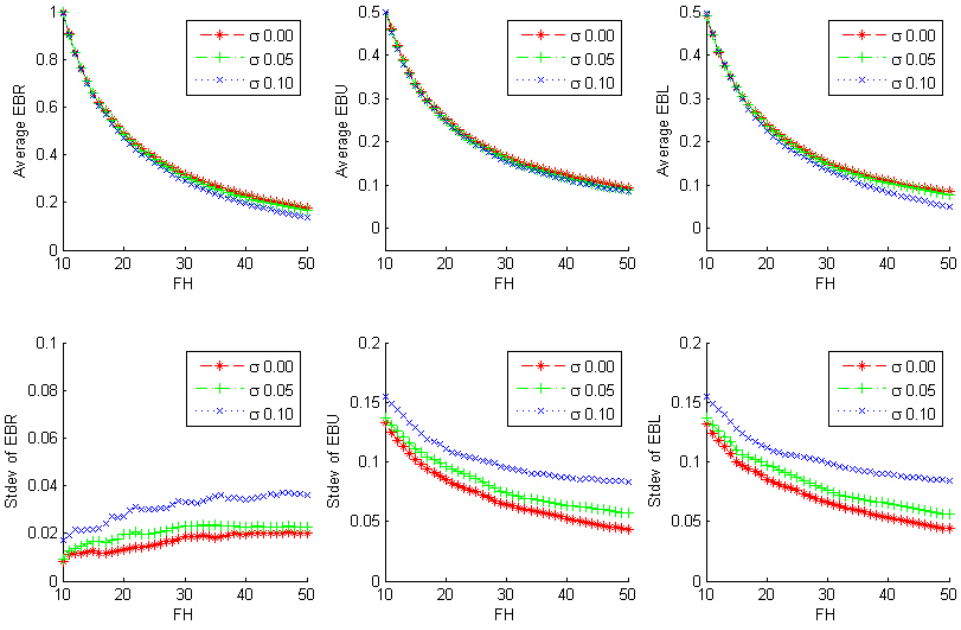

Figure 11. Reservoir storage capacity's effect on error bounds (s = 10.0).

2006] and to set s'_T (equation (3)) as $\underline{s}$ or $\overline{s}$ may become neither necessary nor realistic and EBU and EBL as defined in this paper will exaggerate the actual range of the reservoir release decisions. To regulate reservoirs with large $s/(\mu C_v)$ (e.g., annual and multiannual reservoirs), balancing between water usage within FH and beyond FH, establishing a proper end storage level s'_T becomes more important.

3.5. An Extended Experiment Considering Autoregressive Forecast Uncertainty

[36] Experiment 1–5 adopts an additive forecast uncertainty [*Lettenmaier*, 1984; *Graham and Georgakakos*, 2010; *Zhao et al.*, 2011]. As a comparison, we design an extended experiment with an autoregressive forecast uncertainty incorporating the dependence between streamflow q_i and its forecast x_i [*Weigel et al.*, 2008; *Sankarasubramanian et al.*, 2009b]

$$x_i = \mu_i + \gamma_i(q_i - \mu_i) + \tau_i. \tag{11}$$

In equation (11), i is time index, μ_i is the average of streamflow in period i, γ_i is the correlation between x_i and q_i, and τ_i is the random disturbance with a mean of $(1-\gamma_i)\mu_i$ and a variance of $(1-\gamma_i^2)\mu^2 C_v^2$. For the forecast generated with equation (11), γ_i indicates the forecast skills; $\gamma_i = 1$ implies that $x_i = q_i$ (perfect forecast). In general, we can assume that the forecast skill decreases with FH increase

$$\gamma_i = \max(0, 1 - i\delta) \tag{12}$$

Equation (12) ensures that γ_i is not negative [*Weigel et al.*, 2008]; δ represents the forecast uncertainty magnitude and it is analogy to σ in equation (9).

[37] *Weigel et al.* [2008] proposed the innovative model (10) to evaluate streamflow forecast and suggested that in equation (11), τ_i can be in the form of either a deterministic random disturbance (τ_β) or an ensemble of disturbances $[\tau_1, \tau_2, \ldots, \tau_M]^T$

$$\begin{cases} \tau_i = \tau_\beta \\ \tau_i = \begin{pmatrix} \tau_1 \\ \tau_2 \\ \vdots \\ \tau_M \end{pmatrix} \end{cases}. \tag{13}$$

As shown by *Weigel et al.* [2008], when $\tau_i = \tau_\beta$, $x_i = \mu_i + \gamma_i(q_i - \mu_i) + \tau_\beta$, which represents a deterministic forecast, $\tau_i = \tau_\beta$ cannot interpret the distribution of τ_i and the forecast (x_i) is overconfident; when $\tau_i = [\tau_1, \tau_2, \ldots, \tau_M]^T$, $x_i = \mu_i + \gamma_i(q_i - \mu_i) + [\tau_1, \tau_2, \ldots, \tau_M]^T$, which represents a well dispersed ensemble forecast and can interpret forecast uncertainty well.

[38] This experiment uses δ in equation (12) to indicate the magnitude of forecast uncertainty and equations (11)–(13) to synthesize a forecast, through which the effect of FH and FU on the optimality of r'_1 in both deterministic and ensemble forecast conditions can be examined. We evaluate three levels of δ (0.00, 0.02 and 0.04) and set other parameters used in this experiment the same as those in experiments 1–5. It should be noted that the ensemble forecast corresponds to a stochastic case, for which the monotonicity property between reservoir release and ending storage is adopted and the improved stochastic dynamic programming algorithm proposed in the work of *Zhao et al.* [2012] to handle ensemble forecast is employed. The average and standard deviation of EBR, EBU, and EBL in the deterministic and ensemble forecast cases are plotted in Figure 12 and Figure 13, respectively.

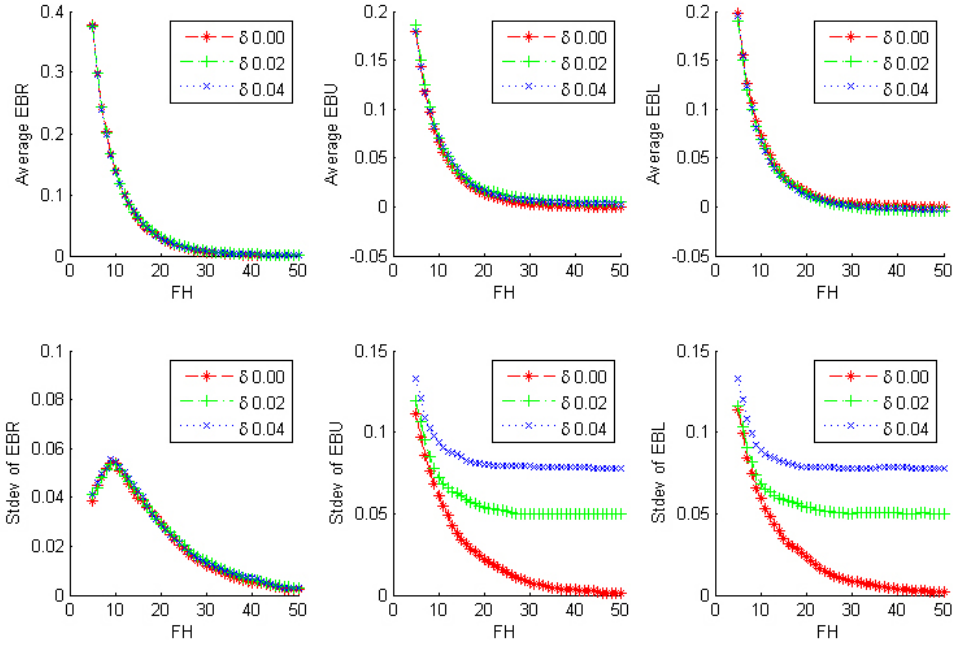

Figure 12. Error bounds under deterministic forecast errors.

[39] As can be seen from Figure 12 and Figure 13, in both deterministic and ensemble forecast cases, the average value and standard deviation of the error bound metrics exhibit a decreasing trend when FH increases. The value of standard deviation of EBR converges to 0 while that of EBU, EBL converges to a certain value depending on FU: a larger FU induces a quicker convergence rate, which again shows the complicating effect of FU and FH and the existence of the EFH as discussed in section 3.2–3.4. At the same FU level, EFH in both deterministic and ensemble forecast cases are in general the same. However, ensemble forecast results in significantly lower standard deviation of EBU and EBL than the deterministic forecast. This shows that an ensemble forecast can be more efficient in guiding reservoir decision making [*Carpenter and Georgakakos*, 2001; *Faber and Stedinger*, 2001; *Valeriano et al.*, 2010; *Zhao et al.*, 2011].

4. A Real-World Case Study

[40] The analysis described above is applied to a real-world case study—the Danjiangkou Reservoir, one of the major reservoirs for water transfer in the central route of the South-North Water Transfer Project (SNWTP) in

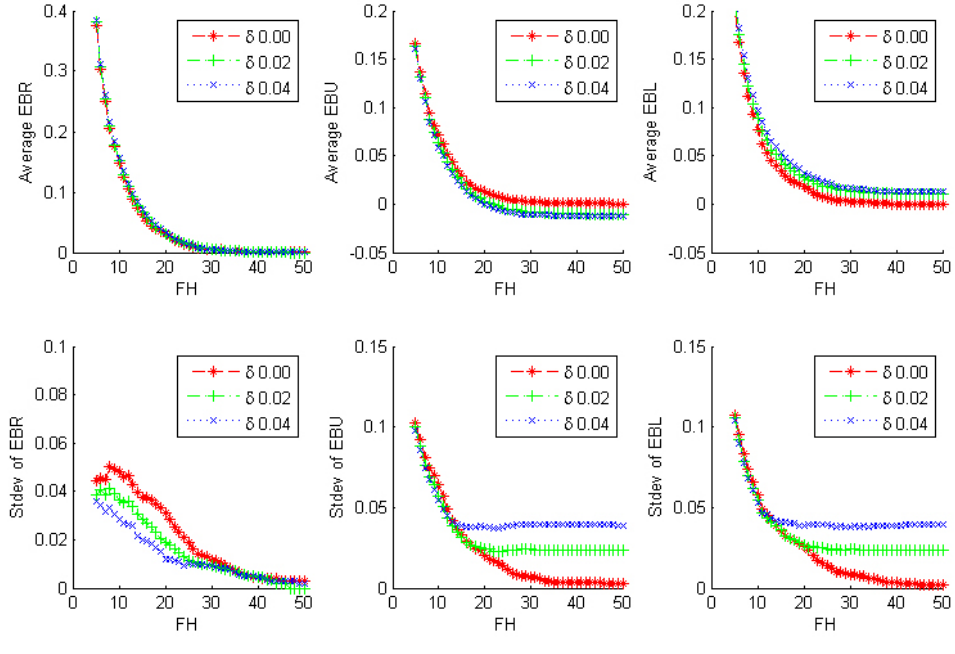

Figure 13. Error bounds under ensemble forecast uncertainties.

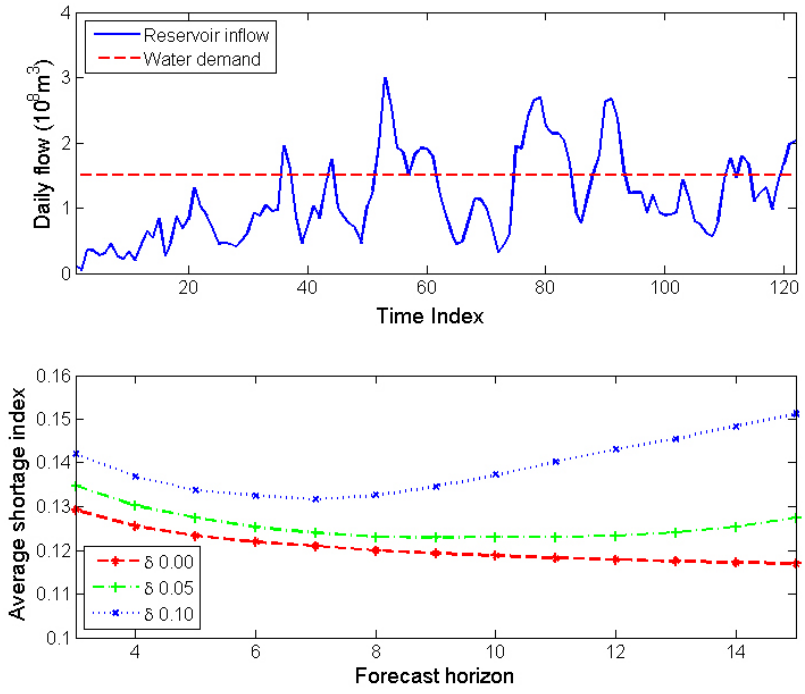

Figure 14. Danjiangkou reservoir water supply operation evaluation under different FU and FH conditions (Note: average shortage index with perfect forecast guided reservoir operation (FH = 122 and δ = 0.00) is 0.116 and that without forecast guided reservoir operation is 0.186).

China. The retrospective analysis period is selected as June 1 to September 30 in 2008 (122 days). The series of inflow and water demand in the period are plotted in the upper part of Figure 14.

[41] The case study focuses on the water supply function of the reservoir and the objective function is chosen as minimizing the shortage index:

$$\min \quad SI = \sum_{i=1}^{122} \left(\frac{TS_i}{TD_i} \right)^2 \tag{14}$$

in which i is the time index (i = 1, 2, ... 122); TD_i is the water demand in period i; TS_i is the water shortage defined as below

$$TS_i = \max(0, TD_i - r_i) \tag{15}$$

The constraints are similar to that in equation (3). $\underline{s}$ and $\overline{s}$ are set as 121.0 $\times$ 10^8 m^3 and 146.6 $\times$ 10^8 m^3, respectively; the release constraint is not considered. Since the reservoir also serves for flood control, as well as water supply, during the study period, the ending storage s'_T is set as the minimum storage ($\underline{s}$) for flood control, 12.1 billion m^3. As s'_T is set as the minimum following the flooding control regulation and r'_1 is the maximum, only EBU described in section 3 is analyzed for the case study.

[42] The autoregressive forecast uncertainty is incorporated into the retrospective analysis in a rolling time window, as shown in Figure 1. In each day, a deterministic streamflow forecast within the FH is generated using equations (11)–(13) and it is assumed that the forecast error τ_i fits a gamma distribution with the mean of $(1 - \gamma_i)\mu_i$ and the variance of $(1 - \gamma_i^2)\mu^2 C_v^2$ [*Sankarasubramanian et al.*, 2009b]. In the rolling horizon reservoir operation (Figure 1), the release decision of the current day determined by the optimization model is implemented, and the reservoir storage is updated to next day. In the numerical experiments, FH is varied from 3 days to 15 days and three δ levels (δ = 0.00, 0.05, and 0.10) are tested. The results that illustrate the relationships between FU, FH and average shortage index are presented in the lower part of Figure 14.

[43] As can be seen from Figure 14, at the same FH level, the lower the FU, the better the reservoir performance; meanwhile, at the same FU level, if there is no uncertainty (δ = 0.00), the longer FH, the better the reservoir performance; while if FU exists, to prolong FH beyond a certain threshold (i.e., EFH) will even decline the reservoir performance. EFH = 12 corresponding to δ = 0.05 and EFH = 7 when δ = 0.10, which verifies that a larger FU ends with a shorter EFH.

5. Discussions and Conclusions

[44] In real-time reservoir operation, FH and FU can affect reservoir release decisions in a complicating manner as the forecast can be too uncertain if it is too long (i.e., information is not reliable) or too short to support decision making effectively. This paper addresses the complicating effect of the two factors using an optimization model established in the framework of rolling horizon decision making. Given a concavity (i.e., diminishing marginal utility) assumption of the reservoir utility function, it is proved that a monotonicity relation exists between the first period (i.e., current) release decision and the ending storage. Based on this property, three error bound metrics are proposed to

evaluate the performance of reservoir operation with an imperfect inflow forecast characterized.

[45] From numerical experiments with a hypothetical reservoir operation model incorporating a synthetic forecast generator, it is found that (1) when FH is short, reservoir decision is primarily controlled by FH and the reservoir performance is improved significantly (error bounds decreases largely) as FH increases; (2) when FH is long, the control factor on reservoir decision is switched to FU, because the inflow information can be too uncertain to guide reservoir operation; (3) at a medium FH, reservoir performance depends on the complicating effect of FU and FH (i.e., less but more reliable versus more but less certain inflow information) and EFH stays with a certain medium level with a balanced level of FU and FH. In general, EFH is shorter with a higher FU but the relation depends on inflow variability and reservoir characteristics.

[46] Numerical experiments also show the impact of the various factors on the EFH. A smaller temporal correlation between FU in single periods results in lower overall FU and consequently more efficient reservoir operation. Lower inflow variability allows a longer timeframe to explore the optimal solution and results in a longer EFH. A reservoir with a large storage loss is less effective at regulating inflow, and inflow information becomes less important. A reservoir with a large storage capacity can regulate inflow through a longer time range. We also verify the complicating effect of FH and FU and illustrate the statistical characteristics of EFH under both deterministic and ensemble forecast cases. Although the ensemble forecast leads to a better reservoir performance, there is not a significant difference between the EFH resulting from the two forecasts, which is probably due to the existence of FU in the two cases.

[47] Moreover, this study shows how to obtain statistical characteristics of EFH through Monte Carlo simulations, as well as identifying the influencing factors of EFH. For a real-world reservoir system, the characteristics of EFH can be identified by retrospective analysis with historical inflow time series and synthetic forecast generators with forecast uncertainty statistics. Given stochastic forecast uncertainty, it is not realistic to identify a deterministic EFH. However, the statistical characteristics of EFH based on retrospective analysis are valuable to real-time reservoir operation.

Appendix A

A1. Theorem

[48] Given a predetermined forecast horizon FH and inflow forecast $[x_1 \quad x_2 \quad \dots \quad x_H]$, if the reservoir release utility function $f_i()$ exhibits a diminishing marginal utility property (i.e., concavity and $f_i''() < 0$), then r'_1 underlying a given s'_T will not increase if s'_T increases.

A2. Proof

[49] This theorem can be proved by the falseness of its counter proposition: for two ending storage levels $s'_{T,1}$, $s'_{T,2}$ of the practical model in equation (3), denoting the corresponding optimal release decision sequences are $R'_1 = [r'_{1,1} \quad r'_{2,1} \quad \dots \quad r'_{H,1}]$, $R'_2 = [r'_{1,2} \quad r'_{2,2} \quad \dots \quad r'_{H,2}]$ respectively, and the corresponding optimal storage sequences are $S'_1 = [s'_{1,1} \quad s'_{2,1} \quad \dots \quad s'_{H,1}]$, $S'_2 = [s'_{1,2} \quad s'_{2,2} \quad \dots \quad s'_{H,2}]$, respectively.

[50] If the counter proposition is true, then there exist two end storage levels $s'_{T,1} < s'_{T,2}$ and

$$r'_{1,1} < r'_{1,2} \tag{A1}$$

[51] By equations (3a), (3b), and (3c), we can deduce that

$$(1-l)^H s_0 + \sum_{i=1}^{H} [(1-l)^{H-i}(x_i - r'_i)] = s'_T. \tag{A2}$$

[52] With equation (A2), we can get

$$\sum_{i=1}^{H} [(1-l)^{H-i}(r'_{i,1} - r'_{i,2})] = s'_{T,2} - s'_{T,1}. \tag{A3}$$

[53] Since $s'_{T,1} < s'_{T,2}$, then

$$\sum_{i=1}^{H} (1-l)^{H-i} r'_{i,1} > \sum_{i=1}^{H} (1-l)^{H-i} r'_{i,2}. \tag{A4}$$

[54] If $r'_{1,1} < r'_{1,2}$, then according to equation (A4), there is at least one integer i $(1 < i \le H)$ satisfying that

$$r'_{i,1} > r'_{i,2}. \tag{A5}$$

[55] Suppose k is the minimum of such integers i and denote

$$\begin{cases} \varepsilon_1 = \min [r'_{1,2} - r'_{1,1}, (1-l)^{1-k}(r'_{k,1} - r'_{k,2})] \\ \varepsilon_k = \min [(1-l)^{k-1}(r'_{1,2} - r'_{1,1}), r'_{k,1} - r'_{k,2}] \end{cases}, \tag{A6}$$

[56] ε_1 and ε_k show a relationship

$$\varepsilon_k = (1-l)^{k-1} \varepsilon_1. \tag{A7}$$

[57] Create a new solution NR'_1 for the end storage level $s'_{T,1}$ as

$$\begin{aligned} NR'_1 &= [\tilde{r}'_{1,1} \quad \dots \quad \tilde{r}'_{k,1} \quad \dots \quad \tilde{r}'_{H,1}] \\ &= [r'_{1,1} + \varepsilon_1 \quad \dots \quad r'_{k,1} - \varepsilon_k \quad \dots \quad r'_{H,1}] \end{aligned}. \tag{A8}$$

[58] NR'_1 will be a feasible solution of the practice model for the following:

[59] 1. Since $\underline{r} \le r'_{1,1} < r'_{1,1} + \varepsilon_1 = \tilde{r}'_{1,1} \le r'_{1,2} \le \overline{r}$ and $\underline{r} \le r'_{k,2} \le r'_{k,1} - \varepsilon_k = \tilde{r}'_{k,1} < r'_{k,1} \le \overline{r}$, the solution NR'_1 satisfies the release constraint;

[60] 2. Denote the storage sequence NS'_1 corresponding to NR'_1 as

$$\begin{aligned} NS'_1 &= [\tilde{s}'_{1,1} \quad \tilde{s}'_{2,1} \quad \dots \quad \tilde{s}'_{k-1,1} \quad \tilde{s}'_{k,1} \quad \dots \quad \tilde{s}'_{H,1}] \\ &= [s'_{1,1} - \varepsilon_1 \quad s'_{2,1} - \varepsilon_2 \quad \dots \quad s'_{k-1,1} - \varepsilon_{k-1} \quad s'_{k,1} \quad \dots \quad s'_{H,1}] \end{aligned} \tag{A9}$$

In equation (A9), $\varepsilon_i = (1-l)^{i-1} \varepsilon_1 \quad (j = 1, \dots, k-1)$. Since $\underline{s} \le s'_{j,2} \le s'_{j,1} - \varepsilon_j = \tilde{s}'_{j,1} < s'_{j,1} \le \overline{s}$ $(j = 1, \dots, k-1)$

and $\tilde{s}'_{j,1} = s'_{j,1}$ $(j = k, \ldots, H)$, the solution NR'_1 also satisfies the storage constraint.

[61] Since R'_1 and NR'_1 are the optimal solution and a feasible solution for $s'_{T,1}$, respectively, we can get

$$\begin{aligned}
&\sum_{i=1}^{H}(1+d)^{1-i} f_i(r'_{i,1}) - \sum_{i=1}^{H}(1+d)^{1-i} f_i(\tilde{r}'_{i,1}) \\
&= f_1(r'_{1,1}) + (1+d)^{1-k} f_k(r'_{k,1}) \\
&\quad - f_1(\tilde{r}'_{1,1}) - (1+d)^{1-k} f_k(\tilde{r}'_{k,1}) \\
&= f_1(r'_{1,1}) + (1+d)^{1-k} f_k(r'_{k,1}) \\
&\quad - f_1(r'_{1,1} + \varepsilon_1) - (1+d)^{1-k} f_k(r'_{k,1} - \varepsilon_k) \\
&> 0
\end{aligned} \tag{A10}$$

[62] Perform the taylor expansion for equation (A10) and omit the second-order items; from this we can derive

$$\left(\frac{1-l}{1+d}\right)^{k-1} \left.\frac{df_k(r)}{dr}\right|_{r'_{k,1}} - \left.\frac{df_1(r)}{dr}\right|_{r'_{1,1}} > 0 \tag{A11}$$

[63] Based on the diminishing marginal utility assumption of $f_i()$, since $r'_{1,1} < r'_{1,2}$ and $r'_{k,1} > r'_{k,2}$, we can get

$$\left.\frac{df_1(r)}{dr}\right|_{r'_{1,2}} < \left.\frac{df_1(r)}{dr}\right|_{r'_{1,1}}, \tag{A12}$$

$$\left.\frac{df_k(r)}{dr}\right|_{r'_{k,2}} > \left.\frac{df_k(r)}{dr}\right|_{r'_{k,1}}, \tag{A13}$$

[64] From equations (A11), (A12), and (A13), we can deduce that

$$\begin{aligned}
&\left(\frac{1-l}{1+d}\right)^{k-1} \left.\frac{df_k(r)}{dr}\right|_{r'_{k,2}} - \left.\frac{df_1(r)}{dr}\right|_{r'_{1,2}} \\
&> \left(\frac{1-l}{1+d}\right)^{k-1} \left.\frac{df_k(r)}{dr}\right|_{r'_{k,1}} - \left.\frac{df_1(r)}{dr}\right|_{r'_{1,1}} \\
&> 0
\end{aligned} \tag{A14}$$

[65] Create a new solution NR'_2 for the end storage level $s'_{T,2}$ as

$$\begin{aligned}
NR'_2 &= [\tilde{r}'_{1,2} \quad \ldots \quad \tilde{r}'_{k,2} \quad \ldots \quad \tilde{r}'_{H,2}] \\
&= [r'_{1,2} - \varepsilon_1 \quad \ldots \quad r'_{k,2} + \varepsilon_k \quad \ldots \quad r'_{H,2}]
\end{aligned}. \tag{A15}$$

NR'_2 is a feasible solution, for which the proof is similar to that of NR'_1.

[66] Make Taylor expansion for $\sum_{i=1}^{H}(1+d)^{1-i} f_i(r'_{i,2}) - \sum_{i=1}^{H}(1+d)^{1-i} f_i(\tilde{r}'_{i,2})$, we can get that

$$\begin{aligned}
&\sum_{i=1}^{N}(1+d)^{1-i} f_i(r'_{i,2}) - \sum_{i=1}^{N}(1+d)^{1-i} f_i(\tilde{r}'_{i,2}) \\
&= f_1(r'_{1,2}) + (1+d)^{1-k} f_k(r'_{k,2}) \\
&\quad - f_1(\tilde{r}'_{1,2}) - (1+d)^{1-k} f_k(\tilde{r}'_{k,2}) \\
&= f_1(r'_{1,2}) + (1+d)^{1-k} f_k(r'_{k,2}) \\
&\quad - f_1(r'_{1,2} - \varepsilon_1) - (1+d)^{1-k} f_k(r'_{k,2} + \varepsilon_k) \\
&\approx -\left(\left(\frac{1-l}{1+d}\right)^{k-1} \left.\frac{df_k(r)}{dr}\right|_{r'_{k,2}} - \left.\frac{df_1(r)}{dr}\right|_{r'_{1,2}}\right)\varepsilon_1
\end{aligned}. \tag{A16}$$

[67] As R'_2 is the optimal solution for $s'_{T,2}$, we can deduce that

$$\left(\frac{1-l}{1+d}\right)^{k-1} \left.\frac{df_k(r)}{dr}\right|_{r'_{k,2}} - \left.\frac{df_1(r)}{dr}\right|_{r'_{1,2}} < 0. \tag{A17}$$

Equations (A17) is a contradiction to equation (A14), so the counter proposition in equation (A1) is false and the theorem is true.

Appendix B

[68] The forecast uncertainty sequence $[\varepsilon_1 \quad \varepsilon_2 \quad \ldots \quad \varepsilon_H]$ contains H (i.e., forecast horizon) elements with increasing standard deviation with forecast lead time (equations (8) and (9)) and a correlation ρ_{error} between forecast errors of two consecutive periods.

[69] We use the variance-covariance matrix of $[\varepsilon_1 \quad \varepsilon_2 \quad \ldots \quad \varepsilon_H]$ to generate this sequence

$$\text{VCV} = \begin{bmatrix}
\varsigma_1^2 & \rho_{\text{error}}\varsigma_1\varsigma_2 & \cdots & 0 & 0 \\
\rho_{\text{error}}\varsigma_1\varsigma_2 & \varsigma_2^2 & \cdots & 0 & 0 \\
\vdots & \vdots & \ddots & \vdots & \vdots \\
0 & 0 & \cdots & \varsigma_{H-1}^2 & \rho_{\text{error}}\varsigma_{H-1}\varsigma_H \\
0 & 0 & \cdots & \rho_{\text{error}}\varsigma_{H-1}\varsigma_H & \varsigma_H^2
\end{bmatrix}. \tag{B1}$$

[70] As the VCV matrix is semidefinite, it can be decomposed into the product of a matrix multiplied by its transpose through Cholesky decomposition, i.e.,

$$\text{VCV} = V * V^T. \tag{B2}$$

[71] Denote $[\theta_1, \theta_2, \ldots, \theta_H]$ as a vector of H independent variables with identical standard Gaussian distribution, then by transposing $[\theta_1, \theta_2, \ldots, \theta_H]$ with V^T, i.e.,

$$[\vartheta_1, \vartheta_2, \ldots, \vartheta_H] = [\theta_1, \theta_2, \ldots, \theta_H]V^T, \tag{B3}$$

we get H new random variables and we can verify that $[\vartheta_1, \vartheta_2, \ldots, \vartheta_H]$ are Gaussian random variables whose variance-covariance matrix is identical to VCV.

[72] Thus by setting

$$[\varepsilon_1 \quad \varepsilon_2 \quad \ldots \quad \varepsilon_H] = [\vartheta_1, \vartheta_2, \ldots, \vartheta_H], \tag{B4}$$

we generate the forecast uncertainty sequence with predefined statistical characteristics.

[73] **Acknowledgments.** We're grateful for the Associate Editor and the three anonymous reviewers for their constructive suggestions, which led major improvements of the paper. This research was partially supported by the National Natural Science Foundation of China (NSFC Grant No. 50928901 and 51025931) and the US National Aeronautics and Space Administration (NASA) grant (Project No. NNX08AL94G). The authors also thank Michelle Miro for editorial assistance to this paper.

References

Ajami, N. K., G. M. Hornberger, and D. L. Sunding (2008), Sustainable water resource management under hydrological uncertainty, *Water Resour. Res.*, *44*, W11406, doi:10.1029/2007WR006736.

Booker, J. F., and J. C. O'Neill (2006), Can reservoir storage be uneconomically large?, *J. Water. Resour. Plan. Manage*, *132*(6), 520–523.

Brooke, A., D. Kendrick, A. Meeraus, and R. Raman (1998), *GAMS: A User's Guide*, GAMS Dev. Corp., Washington, D. C.

Carpenter, T. M., and K. P. Georgakakos (2001), Assessment of Folsom lake response to historical and potential future climate scenarios: 1. Forecasting, *J. Hydrol.*, *249*(1–4), 148–175.

Datta, B., and S. J. Burges (1984), Short-term, single, multiple-purpose reservoir operation – importance of loss functions and forecast errors, *Water Resour. Res.*, *20*(9), 1167–1176.

Draper, A. J., and J. R. Lund (2004), Optimal hedging and carryover storage value, *J. Water. Resour. Plan. Manage.*, *130*(1), 83–87.

Faber, B. A., and J. R. Stedinger (2001), Reservoir optimization using sampling SDP with ensemble streamflow prediction (ESP) forecasts, *J. Hydrol.*, *249*(1–4), 113–133.

Georgakakos, A. P., H. M. Yao, M. G. Mullusky, and K. P. Georgakakos (1998), Impacts of climate variability on the operational forecast and management of the upper Des Moines River basin, *Water Resour. Res.*, *34*(4), 799–821.

Georgakakos, K. P., and N. E. Graham (2008), Potential benefits of seasonal inflow prediction uncertainty for reservoir release decisions, *J. Appl. Meteorol. Climatol.*, *47*(5), 1297–1321.

Graham, N. E., and K. P. Georgakakos (2010), Toward understanding the value of climate information for multiobjective reservoir management under present and future climate and demand scenarios, *J. Appl. Meteorol. Climatol.*, *49*(4), 557–573.

Huang, K., and S. Ahmed (2010), A stochastic programming approach for planning horizons of infinite horizon capacity planning problems, *Eur. J. Oper. Res.*, *200*(1), 74–84.

Huang, W. C., and C. L. Hsieh (2010), Real-time reservoir flood operation during typhoon attacks, *Water Resour. Res.*, *46*, W07528, doi:10.1029/2009WR008422.

Labadie, J. W. (2004), Optimal operation of multireservoir systems: State-of-the-art review, *J. Water. Resour. Plan. Manage.*, *130*(2), 93–111.

Lettenmaier, D. P. (1984), Synthetic streamflow forecast generation, *J. Hydraul Eng.*, *110*(3), 277–289.

Loucks, D. P., J. R. Stedinger, and D. A. Haith (1981), *Water Resource System Planning and Analysis*, Prentice-Hall, Englewood Cliffs, N.J.

Martinez, L., and S. Soares (2002), Comparison between closed-loop and partial open-loop feedback control policies in long term hydrothermal scheduling, *IEEE Trans. Power Syst*, *17*(2), 330–336.

Maurer, E. P., and D. P. Lettenmaier (2003), Predictability of seasonal runoff in the Mississippi River basin, *J. Geophys. Res.*, *108*(D16), 8607, doi:10.1029/2002JD002555.

Maurer, E. P., and D. P. Lettenmaier (2004), Potential effects of long-lead hydrologic predictability on Missouri River main-stem reservoirs, *J. Clim.*, *17*(1), 174–186.

McCollor, D., and R. Stull (2008), Hydrometeorological short-range ensemble forecasts in complex terrain. Part II: Economic evaluation, *Weather Forecast.*, *23*(4), 557–574.

Sankarasubramanian, A., U. Lall, F. A. S. Filho, and A. Sharma (2009a), Improved water allocation utilizing probabilistic climate forecasts: Short-term water contracts in a risk management framework, *Water Resour. Res.*, *45*, W11409, doi:10.1029/2009WR007821.

Sankarasubramanian, A., U. Lall, N. Devineni, and S. Espinueva (2009b), The role of monthly updated climate forecasts in improving intraseasonal water allocation, *J. Appl. Meteorol. Climatol. 48*(7), 1464–1482.

Simonovic, S. P., and D. H. Burn (1989), An improved methodology for short-term operation of a single multipurpose reservoir, *Water Resour. Res.*, *25*(1), 1–8.

Valeriano, O. C. S., T. Koike, K. Yang, and D. W. Yang (2010), Optimal dam operation during flood season using a distributed hydrological model and a heuristic algorithm, *J. Hydrol. Eng.*, *15*(7), 580–586.

Veinott, A. F. (1964), Production planning with convex costs—A parametric study, *Manage. Sci.*, *10*(3), 441–460.

Vogel, R. M., and J. R. Stedinger (1987), Generalized storage reliability yield relationships, *J. Hydrol.*, *89*(3–4), 303–327.

Weigel, A. P., M. A. Liniger, and C. Appenzeller (2008), Can multi-model combination really enhance the prediction skill of probabilistic ensemble forecasts?, *Q. J. R. Meteorol. Soc.*, *134*, 241–260.

Yao, H., and A. Georgakakos (2001), Assessment of Folsom Lake response to historical and potential future climate scenarios 2. Reservoir management, *J. Hydrol.*, *249*(1–4), 176–196.

Yeh, W. W. G. (1985), Reservoir management and operations models—A state-of-the-art review, *Water Resour. Res.*, *21*(12), 1797–1818.

You, J. Y. (2008), Hedging rule for reservoir operation: How much, when and how long to hedge, PhD dissertation, University of Illinois at Urbana Champaign, Champaign, IL.

You, J. Y., and X. Cai (2008a), Determining forecast and decision horizons for reservoir operations under hedging policies, *Water Resour. Res.*, *44*, W11430, doi:10.1029/2008WR006978.

You, J. Y., and X. M. Cai (2008b), Hedging rule for reservoir operations: 1. A theoretical analysis, *Water Resour. Res.*, *44*, W01415, doi:10.1029/2006WR005481.

Zambelli, M. S., I. Luna, and S. Soares (2009), Long-term hydropower scheduling based on deterministic nonlinear optimization and annual inflow forecasting models, paper presented at 2009 IEEE Bucharest Power Tech Conference, IEEE Xplore, Bucharest, Romania.

Zhao, T. T. G., X. M. Cai, and D. W. Yang (2011), Effect of streamflow forecast uncertainty on real-time reservoir operation, *Adv. Water. Resour.*, *34*, 495–504, doi:10.1016/j.advwatres.2011.01.004.

Zhao, T. T. G., X. M. Cai, X. H. Lei, and H. Wang (2012), Improved dynamic programming for reservoir operation optimization with concave utility functions, *J. Water. Resour. Plan. Manage-ASCE*, doi:10.1061/(ASCE)WR.1943-5452.0000205.

X. Cai, Ven Te Chow Hydrosystem Laboratory, Department of Civil and Environmental Engineering, University of Illinois at Urbana Champaign, 301 N. Mathews Ave., Urbana, IL 61801, USA. (xmcai@illinois.edu)

H. Wang, D. Yang, J. Zhao, and T. Zhao, Institute of Hydrology and Water Resources, Department of Hydraulic Engineering, Tsinghua University, Tsinghua Park 1, Beijing, 10084, China.